Compounds with Chelating 3-Dimethylamino-1-propyl Ligands as Chemical Vapor Deposition Precursors. Synthesis and Characterization of $M[(CH_2)_3NMe_2]_2$ Complexes of Nickel(II), Palladium(II), and Platinum(II)

R. Joseph Lastowski,[a] Vincent J. Flores,[a] Laurent Souqui,[b] John R. Abelson,[b] and Gregory S. Girolami*,[a]

[a] School of Chemical Sciences, 600 S. Mathews Avenue, University of Illinois at Urbana-Champaign, Urbana, Illinois 61801, United States

[b] Department of Materials Science and Engineering, 1304 W. Green Street, University of Illinois at Urbana-Champaign, Urbana, Illinois 61801, United States

Graphic for TOC

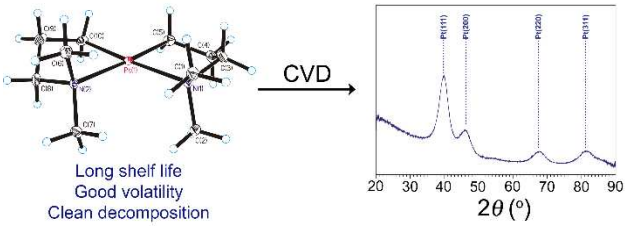

Abstract

We describe the synthesis and characterization of three new square-planar compounds of stoichiometry $M[(CH_2)_3NMe_2]_2$, where M = Ni, Pd, or Pt, each of which contains two chelating 3-dimethylamino-1-propyl ligands. The nickel(II) and palladium(II) compounds decompose above -78 and 0 °C, respectively, but the platinum(II) compound has a thermolysis onset temperature of 130 °C. The Pd and Pt complexes are dynamic in solution: they undergo ring inversion with small free energies of activation of $\Delta G^{\ddagger} = 7.9 \pm 0.1$ and 8.3 ± 0.1 kcal mol^{-1}, respectively, at 298 K. The Pt complex sublimes at 40 °C and 5 mTorr. In benzene solution, the Pt compound thermolyzes primarily through β-hydrogen elimination; 80 ± 10% of the hydrogen atoms and 75 ± 5% of the carbon atoms from the precursor can be accounted for in the byproducts. The thermolysis of **3** in C_6D_6 follows first-order kinetics, with an activation free energy $\Delta G^{\ddagger}$ of 29.9 ± 0.1 kcal mol^{-1} at 110 °C. Under CVD conditions, thin films grown from **3** at 200 °C contain nanocrystalline Pt; analysis of the film growth byproducts suggest that the main decomposition pathway involves β-hydrogen elimination and reductive elimination steps, as seen in solution.

Introduction.

Improvements in the chemical vapor deposition (CVD)[1-4] and atomic layer deposition (ALD)[5-8] of platinum thin films are of interest for multiple applications in the semiconductors,[9-11] computing,[12-14] energy,[15-19] and medical devices industries.[20-22] Organoplatinum compounds have been particularly of interest for the CVD and ALD of platinum,[2, 23-26] and the methylcyclopentadienyl complex $(C_5H_4Me)PtMe_3$ has become the most commonly employed precursor;[27] it has good thermal stability, is stable towards air and water, and has a relatively high vapor pressure.[28] Despite these benefits, $(C_5H_4Me)PtMe_3$ (and other organoplatinum precursors) suffers from long nucleation delays and requires the use of a co-reactant (such as hydrogen, oxygen, oxygen plasma, or ozone) to afford high purity films.[10, 29-31]

Recent work has shown that nucleation delays can be avoided by employing precursors having ligands that can more easily dissociate from the metal center than the cyclopentadienyl and alkyl groups in $(C_5H_4Me)PtMe_3$.[23-24] In this context, we have previously described the compounds *cis*-bis(η^1,η^2-pent-4-en-1-yl)platinum(II) ($Pt[(CH_2)_3CH=CH_2]_2$)[26] and *cis*-bis(η^1,η^2-2,2-dimethylpent-4-en-1-yl)platinum(II) ($Pt[CH_2CMe_2CH_2CH=CH_2]_2$),[23-24] in which the platinum(II) center is bound to two ω-alkenyl ligands that chelate to the metal through one Pt-C bond and one Pt-olefin bond.[23-24, 26] In both compounds, the platinum-bound olefin groups have relatively low dissociation barriers.

The main structural difference between $Pt[(CH_2)_3CH=CH_2]_2$ and $Pt[CH_2CMe_2CH_2CH=CH_2]_2$ is the presence (or absence) of β-hydrogen atoms. Because it is "β-unstabilized", $Pt[(CH_2)_3CH=CH_2]_2$ readily undergoes β-hydrogen elimination to give relatively pure films of platinum (18% carbon) without the need of a co-reactant.[26] But $Pt[(CH_2)_3CH=CH_2]_2$ is too reactive: it slowly decomposes at room temperature and thus is not a practical CVD

precursor. In contrast, in $Pt[CH_2CMe_2CH_2CH=CH_2]_2$ the β-hydrogen elimination pathway is blocked so that this compound is much more thermally stable (thermolysis onset temperature = 145 °C). But owing to the lack of an accessible β-hydrogen elimination pathway, thermolysis occurs by means of ligand fragmentation reactions; the result is that the films contain significant amounts of carbon when deposition is carried out in the absence of a co-reactant.[24]

Here we describe the synthesis and characterization of new compounds of stoichiometry $M[(CH_2)_3NMe_2]_2$ (M = Ni, Pd, and Pt) in which two 3-dimethylamino-1-propyl ligands chelate to the metal through one M-C bond and one M-N bond. These compounds contain β-hydrogen atoms and so should be able to decompose cleanly, but their thermal stabilities should be enhanced owing to the less labile nature of platinum-amine bonds in comparison with platinum-olefin bonds. Solution-phase and static CVD studies combined with thermogravimetric analyses confirm this prediction: the platinum(II) 3-dimethylamino-1-propyl compound has a thermal stability similar to that of the β-stabilized compound $Pt[CH_2CMe_2CH_2CH=CH_2]_2$, but it decomposes primarily through a β-hydrogen elimination mechanism similar to $Pt[(CH_2)_3CH=CH_2]_2$, so that the resulting films are relatively free of carbon.

Results and Discussion.

Synthesis of $M[(CH_2)_3NMe_2]_2$ Compounds. Two reagents have been used in the past to synthesize organometallic compounds containing the 3-dimethylamino-1-propyl anion: (3-dimethylamino-1-propyl)lithium[32-37] and (3-dimethylamino-1-propyl)magnesium chloride.[38-40] We find that the Grignard reagent is more convenient to prepare on larger scales (~40 mmol) from 3-dimethylamino-1-propyl chloride and magnesium turnings.[41]

The reaction of $NiBr_2(dme)_{1.5}$ (dme = 1,2-dimethoxyethane) in thf (tetrahydrofuran) with 2.2 equiv of (3-dimethylamino-1-propyl)magnesium chloride at -78 °C rapidly produces the nickel(II) complex $Ni[(CH_2)_3NMe_2]_2$, **1**, which can be isolated by crystallization from pentane at -78 °C as yellow needles (Scheme 1). Compound **1** rapidly decomposes at temperatures above -78 °C and is sensitive to air and moisture. Similar reactions of $NiBr_2$ with (3-dimethylamino-1-propyl)magnesium chloride at -40 °C produce dark colored mixtures from which **1** is not isolable. In the crystalline form, **1** decomposes over the course of ~ 1 d at -20 °C.

Scheme 1. Synthesis of $M[(CH_2)_3NMe_2]_2$ (M = Ni, Pd, and Pt) compounds.

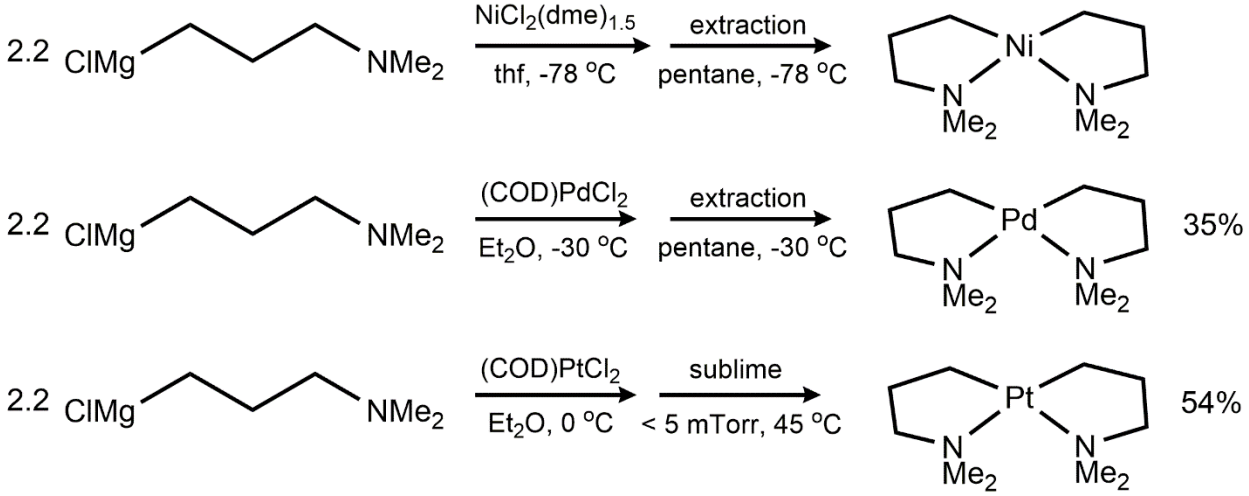

Treatment of $(COD)PdCl_2$ (COD = 1,5-cyclooctadiene) in diethyl ether with 2.2 equiv of (3-dimethylamino-1-propyl)magnesium chloride at -30 °C produces the palladium(II) compound $Pd[(CH_2)_3NMe_2]_2$, **2**, which can be isolated by crystallization from pentane at -20 °C. Solutions of **2** should be handled at 0 °C to minimize decomposition. Similarly, treatment of $(COD)PtCl_2$ in diethyl ether with 2.2 equiv of (3-dimethylamino-1-propyl)magnesium chloride at 0 °C produces the platinum(II) complex $Pt[(CH_2)_3NMe_2]_2$, **3**, which can be isolated either by crystallization from diethyl ether (32% yield) or by sublimation at 45 °C (5 mTorr, 30-50% yield) (Scheme 1). Under

1 atm of N_2, this platinum(II) compound has a thermolysis onset temperature of 130 °C as determined from a thermogravimetric experiment (Figure S31).

Compounds **2** and **3** are moderately soluble in pentane and readily soluble in diethyl ether, benzene, and chloroform. Solid samples of **2** and **3** are moderately air-sensitive and discolor over the course of hours in air.

Crystal Structures of the M[$(CH_2)_3NMe_2$]$_2$ (M = Ni, Pd, and Pt) Compounds. Crystal data and refinement parameters for **1**-**3** are given in Table S1, and relevant bond distances and angles are summarized in Table 1.

All three compounds are isostructural: in each, the metal center is bound to two chelating 3-dimethylamino-1-propyl ligands in a square-planar geometry as commonly seen for d^8 transition metals (Figure 1). The inner C_2N_2 coordination sphere is arranged in a *cis* fashion. In all M[$(CH_2)_3NMe_2$]$_2$ compounds, the two five-membered rings are puckered in opposite directions resulting in C_2 symmetry. Most likely, the *cis* configuration is a consequence of *trans* influences, in which there is an energetic preference for the strongly bonding alkyl groups to be *trans* to the more weakly-bonding amines. The structure of each M[$(CH_2)_3NMe_2$]$_2$ compound is slightly distorted from idealized square planar geometry owing to steric clashing between the NMe_2 groups; these distortions are seen in the obtuse N-M-N angles of 100.62(4), 101.72(4), and 101.45(10)° for **1**, **2**, and **3** respectively.

The M-C and M-N bond lengths in **1**-**3** are similar to those in Ni$(CH_3)_2$(tmed),[42] Pd$(CH_3)_2$(tmed),[43] and Pt$(CH_3)_2$(tmed),[44] respectively. The main structural difference between M[$(CH_2)_3NMe_2$]$_2$ and M$(CH_3)_2$(tmed) (M = Ni, Pd, and Pt) compounds is that the latter are significantly closer to ideal square planar geometry. This difference is best seen in a comparison

of their N-M-N angles: relative to the 101-102° angles found in the current $M[(CH_2)_3NMe_2]_2$ compounds (Table 1), the N-M-N angles in $M(CH_3)_2(tmed)$ (M = Ni, Pd, and Pt) of 85.60(12), 82.73(9), and 83.21(7)°, respectively are significantly closer to the ideal value of 90°

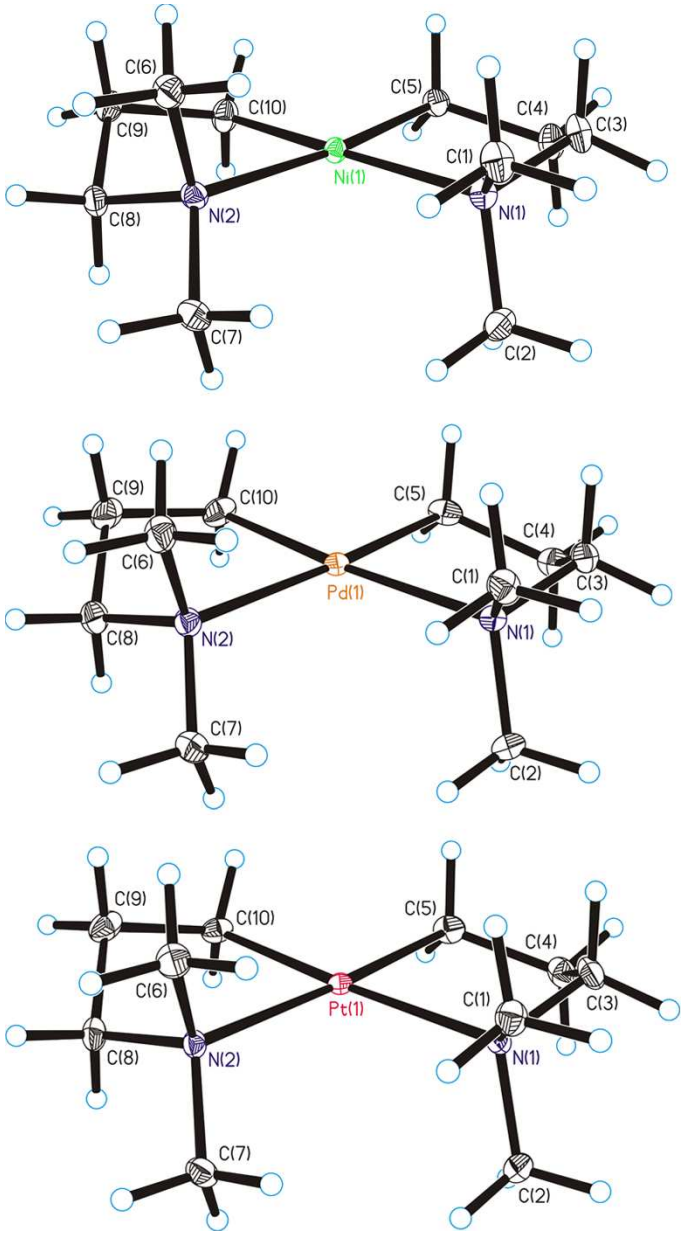

Figure 1. Molecular structures of $Ni[(CH_2)_3NMe_2]_2$ (**1**, top), $Pd[(CH_2)_3NMe_2]_2$ (**2**, center), and $Pt[(CH_2)_3NMe_2]_2$ (**3**, bottom). Ellipsoids are drawn at the 35% probability level, except for the hydrogen atoms, which are represented by arbitrarily sized spheres.

Table 1. Selected distances and angles for $M[(CH_2)_3NMe_2]_2$ compounds (M = Ni, Pd, and Pt).[a]

	$Ni[(CH_2)_3NMe_2]_2$ (**1**)	$Pd[(CH_2)_3NMe_2]_2$ (**2**)	$Pt[(CH_2)_3NMe_2]_2$ (**3**)
M-C (Å)	1.932(1)	2.036(1)	2.035(3)
M-N (Å)	2.092(1)	2.223(1)	2.205(3)
C-M-N_{trans} (°)	172.42(4)	173.81(5)	175.0(1)
C-M-N_{cis} (°)	86.54(4)	84.45(5)	83.5(1)
C-M-C (°)	86.43(5)	89.38(5)	91.5(1)
N-M-N (°)	100.62(4)	101.72(4)	101.5(1)

[a]Some values given are averaged over chemically equivalent bonds.

Solution-phase Dynamic Processes of $Pd[(CH_2)_3NMe_2]_2$ and $Pt[(CH_2)_3NMe_2]_2$. For $Pd[(CH_2)_3NMe_2]_2$ (**2**) and $Pt[(CH_2)_3NMe_2]_2$ (**3**), the crystal structures suggest that the CH_2 protons and NMe_2 methyl groups should be diastereotopic in the ^1H NMR spectrum, owing to the puckering of the chelate rings. However, the room temperature ^1H NMR spectra of compounds **2** and **3** display one sharp resonance for the CH_2 protons and one sharp singlet for the NMe_2 groups (Figures S3 and S6). Similarly, we expect two ^{13}C NMR resonances for NMe_2 groups, but the room temperature $^{13}C\{^1H\}$ NMR spectra of **2** and **3** show only one (Figure 2). These observations suggest that compounds **2** and **3** undergo dynamic processes in solution that exchange the two diastereotopic CH_2 protons and the two diastereotopic NMe_2 methyl groups.

These dynamic processes can be slowed at lower temperatures as shown by the the ^1H NMR spectra of compounds **2** and **3** at -135 °C (Figure S12). Decoalescence of the NMe_2 resonance can be observed by low temperature $^{13}C\{^1H\}$ NMR spectroscopy: at -135 °C the $^{13}C\{^1H\}$ NMR spectra of compounds **2** and **3** display two singlets (with a 1:1 intensity ratio) corresponding to the two diastereotopic NMe_2 methyl groups (Figure 2). These two singlets are

somewhat broad because even at -135 °C the temperature is not low enough for the exchange process to be in the slow-exchange limit.

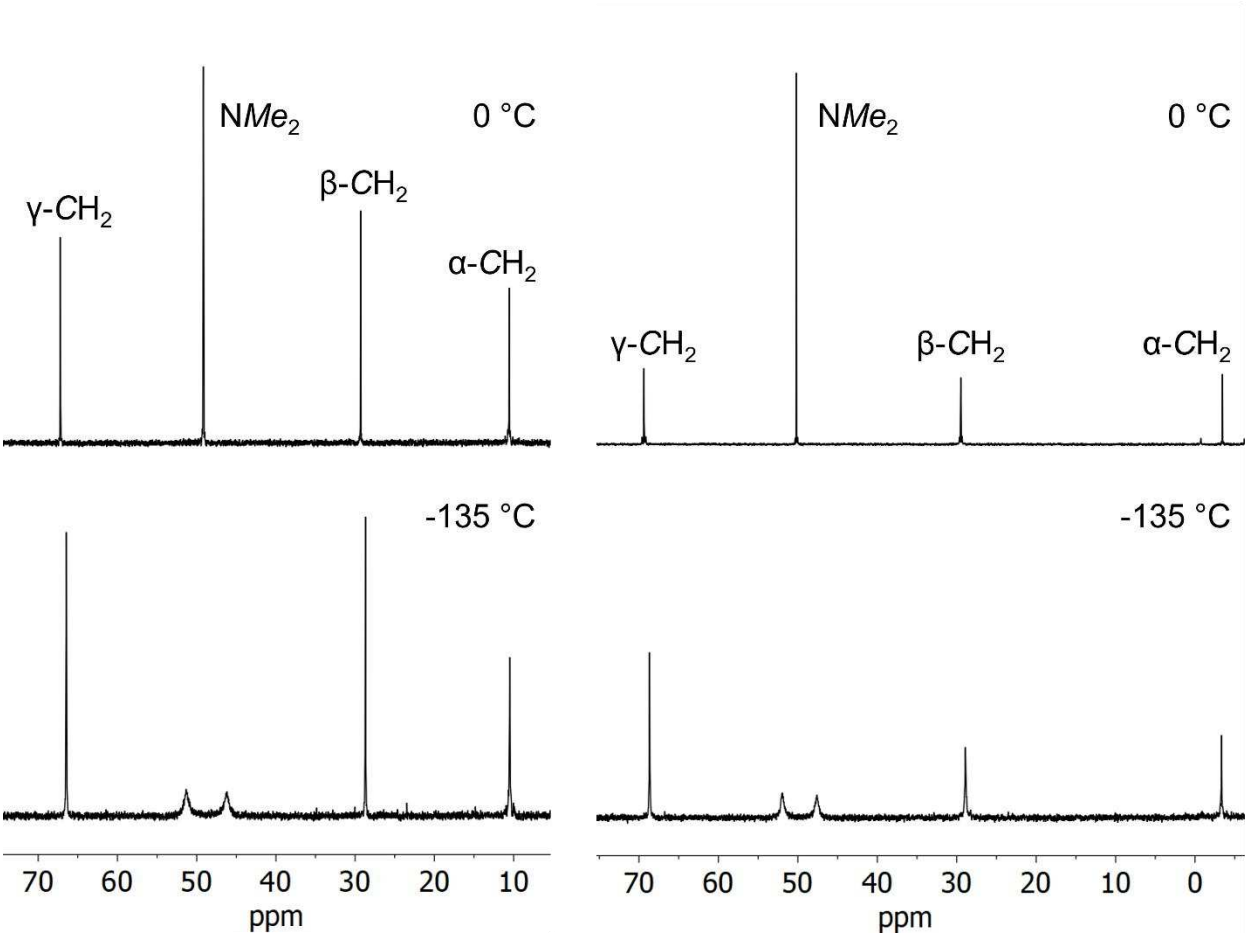

Figure 2. $^{13}C\{^{1}H\}$NMR spectra of $Pd[(CH_2)_3NMe_2]_2$ (**2**, left) and $Pt[(CH_2)_3NMe_2]_2$ (**3**, right) in $CDFCl_2$ at 0 °C (top) and -135 °C (bottom) in $CDFCl_2$.

Computer simulations (WinDNMR)[45] of the variable-temperature $^{13}C\{^{1}H\}$ NMR spectra of **2** and **3** afford rates for the dynamic exchange processes at various temperatures (Figure 3, Table S2). An Eyring plot of the exchange process rates for the palladium compound **2** at thirteen different temperatures between -99 and -135 °C gives the activation parameters $\Delta H^{\ddagger} = 4.9 \pm 0.3$ kcal mol^{-1} and $\Delta S^{\ddagger} = -9.9 \pm 1.9$ cal mol^{-1} K^{-1} (Figure S10). Similarly, an Eyring plot of the exchange rates for the platinum compound **3** at twelve different temperatures between -99 and -135 °C gives

the activation parameters $\Delta H^{\ddagger}$ = 4.7 ± 0.2 kcal mol^{-1} and $\Delta S^{\ddagger}$ = -12.1 ± 1.6 cal mol^{-1} K^{-1} (Figure S10). These parameters correspond to free energies of activation for **2** and **3** of $\Delta G^{\ddagger}$ = 7.9 ± 0.1 and 8.3 ± 0.1 kcal mol^{-1}, respectively, at 298 K.

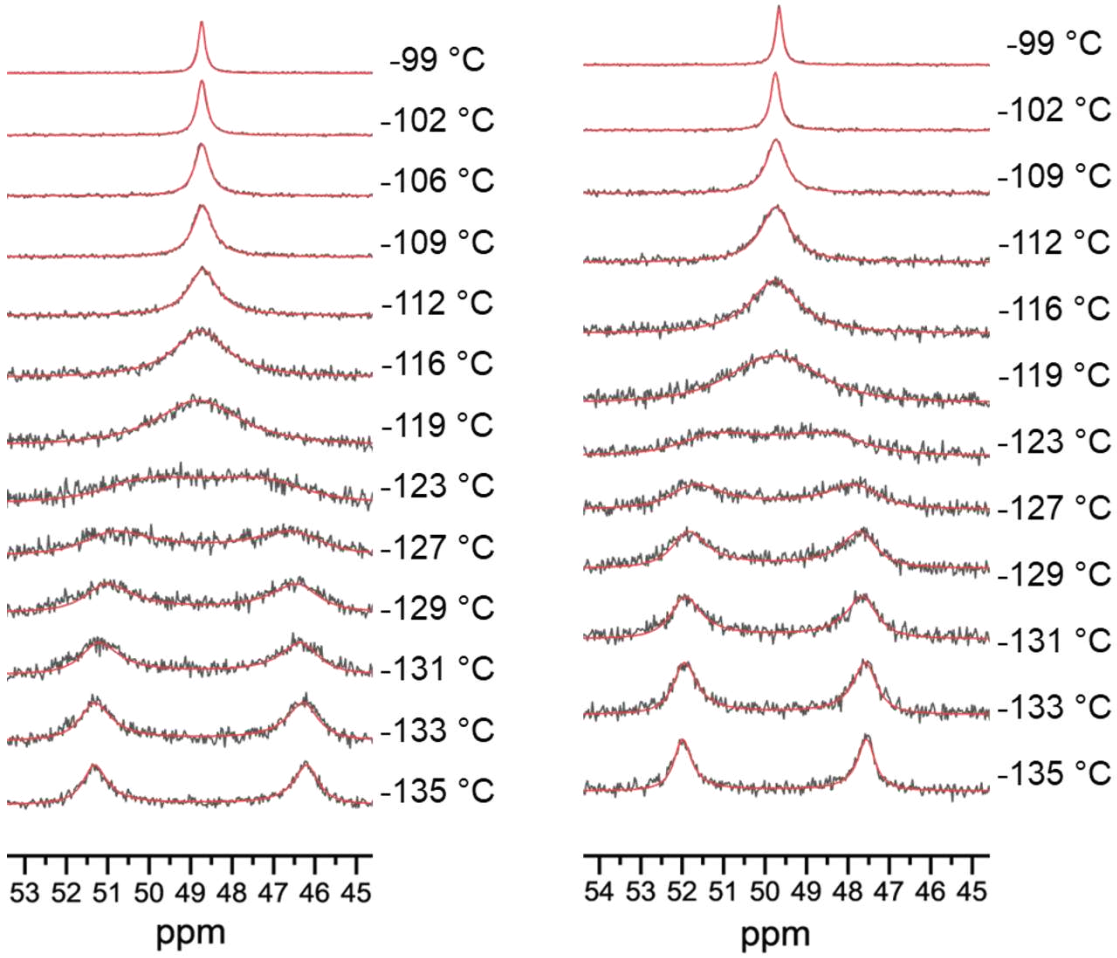

Figure 3. Variable-temperature $^{13}C\{^{1}H\}$ NMR spectra (black) of the methyl resonances of **2** (left) and **3** (right) in $CDFCl_2$, overlaid with simulated spectra (red) at each temperature.

Two mechanisms for the exchange of methylene protons in compounds **2** and **3** are most likely: 1) a dissociative mechanism in which the M-N bond of one ligand breaks, the ligand backbone changes conformation, and the NMe_2 group reassociates, and 2) a non-dissociative mechanism that proceeds through a ring flip (also called ring inversion), similar to the chair-chair

interconversion in cyclohexane. The small positive enthalpies and small negative entropies of measured for **2** and **3** are more consistent with the non-dissociative mechanism. This conclusion is supported by DFT calculations (see Supporting Information) of the Pt compound **3**, which show that the ring inversion mechanism proceeds through a transition state with a relative free energy of 6.4 kcal mol^{-1} at 298 K; this energy is in reasonable agreement with the measured value of $\Delta G^{\ddagger}$ = 8.3 ± 0.1 kcal mol^{-1} for **3**.

Solution-phase Thermolysis of Pt[(CH$_2$)$_3$NMe$_2$]$_2$. To investigate how Pt[(CH$_2$)$_3$NMe$_2$]$_2$, **3**, decomposes in solution, we carried out thermolysis studies in deuterobenzene in sealed NMR tubes. In all thermolysis studies, the initial concentration of **3** was ~0.1 M, and a drop of mercury was added to inhibit any surface reactions between colloidal platinum and thermolysis products.[46] The thermolysis rate of **3** in C_6D_6 becomes significant only above ~90 °C.

Scheme 2. Stoichiometries of products generated upon thermolysis of Pt[(CH$_2$)$_3$NMe$_2$]$_2$ (**3**) at 120 °C in C_6D_6.

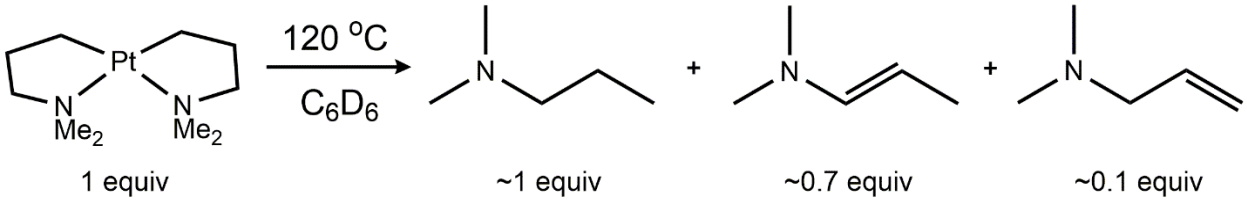

Thermolysis of **3** at 100, 110, and 120 °C in C_6D_6 over 10-35 hours produces a brown solution (due to the formation of colloidal Pt) and a metallic mirror on the inside of the NMR tube. The same three major organic products are generated at each temperature: the ligand hydrogenation product dimethyl(*n*-propyl)amine, and the isomeric ligand dehydrogenation products (*E*)-dimethyl(1-propenyl)amine, and dimethyl(allyl)amine (Scheme 2, Figure S20). The identities of the byproducts and their ratio are consistent with β-hydrogen elimination from **3** to form (initially) dimethyl(allyl)amine and a platinium(II) hydrido aminopropyl intermediate,

followed by reductive elimination from the latter to form dimethyl(propyl)amine and Pt^0. Presumably, the initial β-hydrogen elimination product dimethyl(allyl)amine slowly isomerizes – in the presence of Pt^0 at elevated temperature over the long residence times in the NMR tube – to the more thermodynamically stable isomer (*E*)-dimethyl(1-propenyl)amine. At each temperature, the ratio of hydrogenated byproducts to dehydrogenated byproducts is 1 : 0.8-0.9. Little H/D exchange is observed between the thermolysis products of **3** and C_6D_6, as shown by the ^2H NMR spectra of the organic products (Figure S24).

Throughout each thermolysis experiment, ~80% ± 10% of all protons and 75 ± 5% of all carbon atoms (approximately all of which are attributed to the thermolysis products described above) can be accounted for by ^1H NMR spectroscopy, indicating that ~20% of the ligand groups of **3** present at the beginning of thermolysis are incorporated either into the film formed on the inside of the NMR tube or into the colloidal black precipitate (See Supporting Information). No platinum-containing thermolysis products could be detected by ^{195}Pt NMR spectroscopy.

The thermolysis of **3** in C_6D_6 follows first-order kinetics, with a rate constant at 110 °C of $k = 7.1 \pm 0.5 \times 10^{-5}$ sec^{-1} (Figure S14) This rate corresponds to an activation free energy $\Delta G^{\ddagger}$ of 29.9 ± 0.1 kcal mol^{-1},

Hot Stage Static Chemical Vapor Deposition of Thin Films from $Pt[(CH_2)_3NMe_2]_2$. To obtain information about thin films deposited from $Pt[(CH_2)_3NMe_2]_2$, **3**, and the byproducts that are produced, CVD experiments were performed in a static vacuum (~10 mTorr) hot stage deposition system equipped with a liquid nitrogen cooled NMR tube (to trap volatile byproducts).[24, 47] The precursor reservoir was maintained between 60 and 70 °C to achieve reasonable growth rates, and the gaseous precursor was passed over a Si(100) wafer heated to 200 ± 10 °C. The resulting films were smooth and reflective. GI-XRD analysis of films grown from **3**

shows that Pt is in fact the only crystalline phase detected (Figure 4); crystallite sizes were determined to range from 3.7 to 4.9 nm (see Supporting Information).

The ^{1}H NMR spectrum of the collected volatile byproducts shows that the major products generated during film growth from **3** are dimethyl(*n*-propyl)amine, (*E*)-dimethyl(1-propenyl)amine, and dimethyl(allyl)amine (Figure S27), which are the same byproducts detected from the solution-phase thermolysis of **3**. Small amounts of several additional species are produced in the CVD experiments that are not observed during solution phase thermolysis: propylene, dimethylamine, *N*-methylpyrrole, and dihydrogen. These additional products probably result from Pt-catalyzed side reactions: propylene and dimethylamine can be formed by the scission of a C-N bond of dimethyl(*n*-propyl)amine, and *N*-methylpyrrole can be formed by dehydrogenative cyclization of dimethyl(1-propenyl)amine or dimethyl(allyl)amine, via activation of the C-H bonds of one of the *N*-methyl groups.

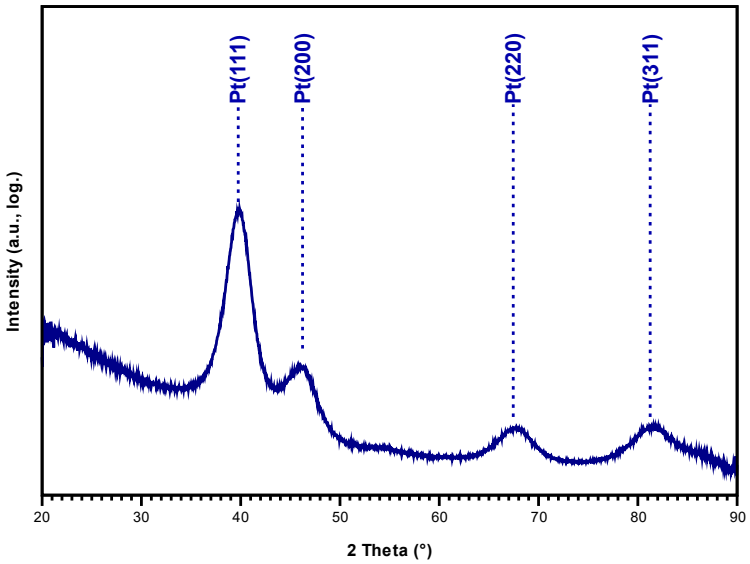

Figure 4. Grazing incidence XRD spectrum of a Pt film grown from $Pt[(CH_2)_3NMe_2]_2$, **3**, on a Si(100) wafer at 200 °C in a static hot stage CVD system. The film contains nanocrystalline platinum. The 2θ values match with the literature report.[24]

For every one equiv of dimethyl(*n*-propyl)amine that is produced during film growth from **3**, 0.36 equiv of dimethyl(1-propenyl)amine, 0.21 equiv of dimethyl(allyl)amine, 0.26 equiv of propylene, 0.21 equiv of dimethylamine, and 0.08 equiv of *N*-methylpyrrole are produced (Scheme 3). These observations in total suggest that the β-hydrogen elimination/reductive elimination mechanism discussed above is the main decomposition pathway for **3** under CVD conditions.[48]

Scheme 3. Ratios of the product distribution produced by thermolysis of $Pt[(CH_2)_3NMe_2]_2$ (**3**) at 200 °C under static CVD conditions.

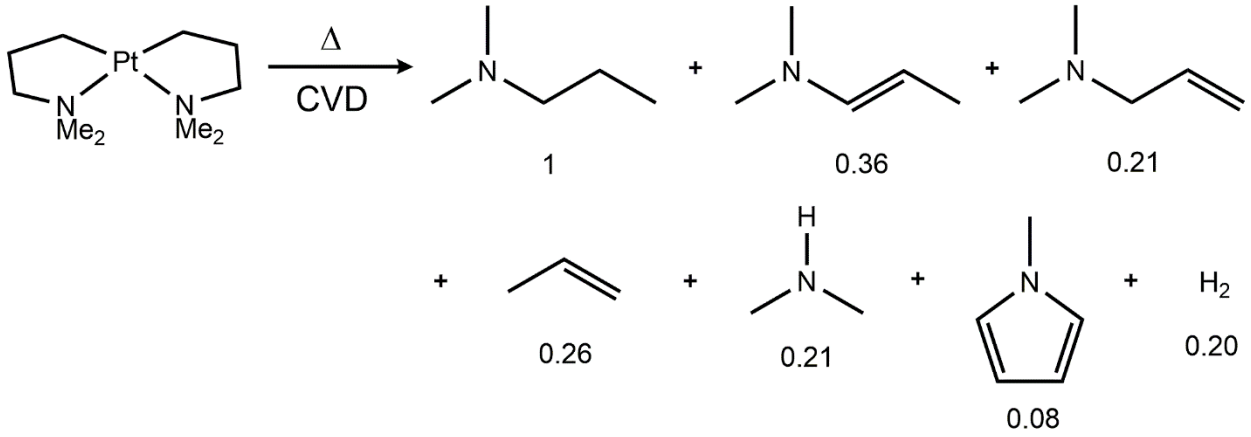

Comparison of $Pt[(CH_2)_3NMe_2]_2$ with $Pt[(CH_2)_3CH=CH_2]_2$ and $Pt[CH_2CMe_2CH_2CH=CH_2]_2$. As mentioned in the introduction, we have previously described two platinum(II) pentenyl complexes that serve as CVD precursors to platinum metal: $Pt[(CH_2)_3CH=CH_2]_2$,[26] and $Pt[CH_2CMe_2CH_2CH=CH_2]_2$.[23-24] Compared with these compounds, the new species described here, $Pt[(CH_2)_3NMe_2]_2$ (**3**), differs in that the neutral Lewis base donor is an amine vs. an olefin in $Pt[(CH_2)_3CH=CH_2]_2$ and $Pt[CH_2CMe_2CH_2CH=CH_2]_2$. The three compounds also differ in whether or not they possess β-hydrogen atoms on the alkyl chain. These variables should affect the thermal stabilities of the compounds and the mechanisms by which they transform into platinum.

The "β-unstabilized" alkyl compound $Pt[(CH_2)_3CH=CH_2]_2$ readily thermolyzes to afford platinum films by a β-hydrogen elimination/reductive elimination process, but the barrier for β-hydrogen elimination is low enough that the compound slowly decomposes at room temperature.[26] As a result, it is not a practical choice as a CVD precursor. In contrast, the "β-stabilized" alkyl compound $Pt[CH_2CMe_2CH_2CH=CH_2]_2$ is much more thermally stable, but because it cannot decompose via β-hydrogen elimination; thermolysis of $Pt[CH_2CMe_2CH_2CH=CH_2]_2$ occurs through a number of higher-energy ligand rearrangements that result in carbon contamination in the films (a defect that can be remedied, however, by addition of co-reactants such as oxygen).[23-24]

The new compound $Pt[(CH_2)_3NMe_2]_2$ (**3**) combines the best aspects of these two platinum pentenyl compounds. Like $Pt[(CH_2)_3CH=CH_2]_2$, compound **3** decomposes mainly through a β-hydrogen elimination/reductive elimination pathway, and almost all of the hydrogen and carbon atoms initially present in the precursor can be accounted for among the organic byproducts (80 ± 10% for **3** and 85% for $Pt[(CH_2)_3CH=CH_2]_2$, compared to 55% for $Pt[CH_2CMe_2CH_2CH=CH_2]_2$ under similar conditions). As a result, the platinum films generated are relatively free of carbon. Unlike $Pt[(CH_2)_3CH=CH_2]_2$, however, compound **3** is thermally stable at room temperature for long periods: its thermolysis onset temperature of 130 °C (Figure S31) is much more similar to that of 145 °C seen for the "β-stabilized" alkyl $Pt[CH_2CMe_2CH_2CH=CH_2]_2$.[24] We attribute the high thermal stability of **3** to the strong Pt-N bond formed to the amine donors of the 3-dimethylamino-1-propyl ligands: β-hydrogen elimination can occur from **3** only after one of the Pt-N bonds is broken.[26, 49-51]

Concluding Remarks.

Compounds of stoichiometry $M[(CH_2)_3NMe_2]_2$, where M = Ni, Pd, or Pt, have been synthesized and characterized in which the metal centers adopt square-planar coordination geometries as expected for low-spin d^8 transition metals. The nickel(II) compound **1** is very unstable thermally, and could be characterized only by crystallography. The palladium(II) and platinum(II) compounds **2** and **3** are fluxional in solution: the five-membered rings formed by the 3-dimethylamino-1-propyl ligands engage in a ring flip process with barriers of $\Delta G^{\ddagger}_{298\ K} = 7.9 \pm 0.1$ and 8.3 ± 0.1 kcal mol^{-1}, respectively.

Thermolysis of **3** in C_6D_6 produces dimethyl(*n*-propyl)amine, dimethyl(allyl)amine, and (*E*)-dimethyl(1-propenyl)amine; these products are formed from **3** through a β-hydrogen elimination / reductive elimination mechanism. Thermolysis of **3** under static CVD conditions produces the products above as well as small amounts of propylene, dimethylamine, *N*-methylpyrrole, and dihydrogen. These additional products are undoubtedly generated by platinum-catalyzed reactions of adsorbed dimethyl(allyl)amine and (*E*)-dimethyl(1-propenyl)amine.

Throughout solution-phase thermolyses of **3**, 80 ± 10% of the protons and 75 ± 5% of the carbon atoms initially present in the precursor can be accounted for among the organic byproducts, indicating that relatively few atoms from the 3-dimethylamino-1-propyl ligands are incorporated into the deposited platinum. GI-XRD analysis of a film grown from **3** shows that platinum is the only crystalline phase present. The clean decomposition pathway and high thermal stability of **3** make it a potentially useful new CVD precursor for platinum metal.

Of the several CVD precursors that have been used to grow Pt thin films, the cyclopentadienyl compound $(C_5H_4Me)PtMe_3$ is the most commonly employed.[52] One difference

between **3** and $(C_5H_4Me)PtMe_3$ is that only **3** is able to undergo a low-energy β-hydrogen elimination reaction, which enables many of the carbon atoms to be carried away as volatile byproducts. As a result, **3** affords cleaner and smoother Pt films than $(C_5H_4Me)PtMe_3$ in the absence of a co-reactant.[24] Although the presence of β-hydrogen atoms in platinum(II) compounds tends to reduce the thermal stability, compound **3** has a decomposition onset temperature (130 °C) owing to the need to break at least one strong Pt-N bond before the β-hydrogen elimination mechanism can take place.[26, 49-51] This temperature is high enough that the compound can be handled without decomposition, but low enough that platinum films can be grown at relatively low temperatures.

Experimental Section

All manipulations were carried out under argon or in vacuum using standard Schlenk and glovebox techniques unless otherwise specified. All glassware was oven-dried before use, assembled hot, and cooled under vacuum. Solvents were distilled under nitrogen from sodium/benzophenone (pentane, diethyl ether, and tetrahydrofuran) and sparged with argon immediately before use. 3-Dimethylamino-1-propyl chloride (Ambeed) was stored at -78 °C to prevent it from polymerizing.[53] 3-Dimethylamino-1-propylmagnesium chloride,[41] $NiBr_2(dme)_{1.5}$,[54] $(COD)PdCl_2$,[55] $(COD)PtCl_2$,[56] and $CDFCl_2$[57] were prepared according to literature procedures. 3- Benzene-d_6 (Cambridge Isotope Laboratories) was distilled from calcium hydride under argon and stored over 3 Å molecular sieves.

Elemental analyses were carried out by the University of Illinois Microanalytical Laboratory. FTIR spectra were acquired on a Thermo Nicolet IR200 spectrometer as mineral oil

mulls between KBr plates and processed using the OMNIC™ software package with automatic baseline corrections. The ^{1}H and $^{13}C\{^{1}H\}$ NMR data were collected on a B600 Bruker NEO instrument at 14.1 T or a Varian Unity Inova 500 instrument at 11.7 T, and the ^{195}Pt and variable temperature ^{1}H and $^{13}C\{^{1}H\}$ NMR data were collected on a Varian Unity Inova 600 instrument at 14.1 T. Low-temperature NMR data were collected in $CDFCl_2$. Chemical shifts are reported in δ units (positive shifts to high frequency) relative to $SiMe_4$ (^{1}H, ^{13}C) by assigning appropriate shifts to solvent peaks, or to an external standard of K_2PtCl_6 (^{195}Pt) by sample replacement. X-ray crystallographic data were collected by the staff of the G. L. Clark X-ray Laboratory at the University of Illinois. Errors in the values of $\Delta H^{\ddagger}$ and $\Delta S^{\ddagger}$ from Eyring plots were determined from propagation of error formulae.[58] Thermogravimetric analysis (TGA) data were collected on a TA Instruments Q50 TGA system. GI-XRD data were collected on a Bruker D8 ADVANCE Plus diffractometer equipped with a Cu X-ray anode, a Göbel mirror to obtain a parallel beam, a 2-mm divergence slit on the primary side, 2.5° Soller slits on the secondary side, and an EIGER2 R 500 K detector. A low background single-crystal sapphire was used as sample holder. The incident angle α was fixed at 1° for the GI-XRD measurement. The estimation of crystallite size was derived from a 2θ/ω scan of the same film, using the Scherrer constant for *hkl* assuming cubic crystallites, Gaussian line shapes (fit using the Fityk software) and with an instrumental broadening of 0.05°.

Bis(3-dimethylamino-1-propyl)nickel(II). Ni[$(CH_2)_3NMe_2$]$_2$, 1. To a stirred suspension of $NiBr_2(dme)_{1.5}$ (250 mg, 0.71 mmol) in thf (10 mL) at -78 °C was added dropwise dimethylamino-1-propylmagnesium chloride (2.0 mL of a 0.8 M solution in thf, 1.60 mmol). The resulting mixture was stirred for 1 h at -78 °C to afford a yellow solution and gray solids. The following steps must be performed quickly to minimize the amount of decomposition of **1**. Volatile material was removed from the mixture as it was warmed to 0 °C under vacuum. The residue was

extracted at 0 °C with diethyl ether (40 mL), and the yellow extract was filtered into a receiving flask maintained at 0 °C. Volatile material was removed from the yellow filtrate at 0 °C to afford a mixture of yellow and black solids. The residue was extracted at 0 °C with pentane (40 mL) and the yellow extract was filtered into a receiving flask maintained at 0 °C. The filtrate was concentrated to ca. 20 mL and cooled to -78 °C to precipitate a mixture and yellow and brown solids. The yellow supernatant was decanted while the source and receiving flasks were maintained at -78 °C, and the decantate was concentrated to ca. 10 mL and kept at -78 °C overnight. This step was repeated until brown solids no longer precipitated and yellow needles formed instead. The needles were studied by X-ray diffraction but further characterization of this compound was impeded by its thermal instability.

Bis(3-dimethylamino-1-propyl)palladium(II). $Pd[(CH_2)_3NMe_2]_2$, 2. To a stirred suspension of $(COD)PdCl_2$ (209 mg, 0.73 mmol) in diethyl ether (30 mL) at -30 °C was added dropwise dimethylamino-1-propylmagnesium chloride (2.0 mL of a 0.8 M solution in thf, 1.60 mmol), and the resulting mixture was stirred for 1.25 h at -30 °C. The pale-yellow solution was filtered into a receiving flask that had been precooled to 0 °C, the filtration residue was extracted at 0 °C with diethyl ether (10 mL), and this extract was filtered into the same precooled receiver. Volatile material was removed from the combined extracts at 0 °C. The residue was extracted with pentane (1 × 30 mL, 1 × 15 mL) at 0 °C, and the extracts were filtered into a receiver that had been precooled to 0 °C. The extracts were concentrated to ca. 35 mL at 0 °C and cooled to -20 °C overnight to produce colorless needles. The needles were collected by decantation at 0 °C and dried under vacuum. Two more crops of colorless solids could be obtained by concentrating the decantate at 0 °C and cooling it to -20 °C. Yield: 71 mg (35%). Anal. Calc. for $PdN_2C_{10}H_{24}$: C, 43.1; H, 8.8; N, 10.1. Found: C, 43.1; H, 8.7; N, 9.9. ^1H NMR (C_6D_6, 25 °C, 600.1 MHz): δ 2.05

(t, $^{3}J_{HH}$ = 5.5 Hz, 4 H, γ-CH_2), 2.04 (s, 12 H, NMe_2), 1.70 ("q", "*J*" = 6.0 Hz, 4 H, β-CH_2), 1.64 ("t", "*J*" = 6.2 Hz, 4 H, α-CH_2). $^{13}C\{^{1}H\}$ NMR (C_6D_6, 25 °C, 125.8 MHz): δ 66.9 (s, γ-CH_2), 48.5 (s, NMe_2), 29.8 (s, β-CH_2), 10.7 (s, α-CH_2). IR (cm^{-1}): 2995 m, 2704 w, 2671 w, 2621 w, 1402 m, 1363 m, 1315 s, 1277 m, 1244 sh, 1232 s, 1198 m, 1163 s, 1105 m, 1095 sh, 1066 m, 1043 m, 1018 s, 974 s, 960 m, 908 s, 893 sh, 883 w, 723 sh, 706 m, 565 m, 544 m, 509 s, 465 m, 444 w, 436 w. Single crystals suitable for X-ray diffraction were grown by cooling a concentrated pentane solution to -20 °C.

Bis(3-dimethylamino-1-propyl)platinum(II). $Pt[(CH_2)_3NMe_2]_2$, 3. To a stirred suspension of (COD)$PtCl_2$ (300 mg, 0.80 mmol) in diethyl ether (40 mL) at 0 °C was added dropwise dimethylamino-1-propylmagnesium chloride (2.9 mL of a 0.6 M solution in thf, 1.8 mmol), and the mixture was stirred for 2 h at 0 °C. The colorless solution was filtered into a receiving flask, the colorless filtration residue was extracted with diethyl ether (10 mL), and the extract was filtered into the same receiver. Volatile material was removed from the combined filtrates under vacuum, the colorless residue was extracted with diethyl ether (1 × 40 mL, 1 × mL), and the extracts were filtered and combined. The extracts were concentrated to ca. 10 mL under vacuum and cooled to -20 °C overnight to produce colorless needles, which were collected by decantation and dried under vacuum. The supernatant was concentrated to ca. 5 mL to produce a second batch of needles. Yield: 93 mg (32%). The title compound can also be sublimed from the filtered reaction mixture (45 °C, 5 mTorr) in yields of 30-50%. Anal. Calc. for $PtN_2C_{10}H_{24}$: C, 32.7; H, 6.6; N, 7.6. Found: C, 32.5; H, 6.6; N, 7.3. ^{1}H NMR (C_6D_6, 25 °C, 600.1 MHz): δ 2.21 (s, 12 H, NMe_2), ~2.21 (t, overlaps with NMe_2 resonance, $^{3}J_{HH}$ = 5.9 Hz, $^{2}J_{PtH}$ = 76 Hz, 4 H, α-CH_2), 2.21 (t, $^{3}J_{HH}$ = 5.9 Hz, $^{3}J_{PtH}$ = 27 Hz, 4 H, γ-CH_2), 1.43 ("q", $^{3}J_{PtH}$ = 133 Hz, 4 H, β-CH_2). $^{13}C\{^{1}H\}$ NMR (C_6D_6, 25 °C, 125.8 MHz): δ 69.02 (s, $^{2}J_{PtC}$ = 70 Hz, γ-CH_2), 49.47 (s, NMe_2), 29.95 (s, $^{2}J_{PtC}$

= 56 Hz, β-CH_2), -3.54 (s, $^1J_{PtC}$ = 851 Hz). ^{195}Pt NMR (C_6D_6, 25 °C, 128.9 MHz): δ 3803.33 (s, fwhm = 300 Hz). IR (cm^{-1}): 3001 m, 2792 s, 2781 sh, 1400 w, 1315 w, 1277 w, 1263 w, 1246 w, 1232 m, 1205 m, 1171 s, 1126 w, 1109 m, 1039 m, 1014 s, 968 s, 949 sh, 920 s, 887 w, 845 w, 783 s, 748 w, 721 w, 667 w, 592 w, 577 m, 553 w, 530 m, 480 m, 472 sh, 459 w, 444 w, 418 m.

Computational Details. Geometry optimizations and frequency calculations were performed with the Gaussian 16 program package[59] using the B3LYP[60-61] functional and def2-TZVPP basis set[62-63] for all atoms. Grimme's D3 empirical dispersion correction[64] was applied with Becke-Johnson (BJ) damping,[65] and solvent field corrections were employed using the conductor-like polarizable continuum model[66] with default parameters for chloroform. Transition state searches were performed by searching for a saddle point based on an initial guess geometry using the B3LYP functional, the def2-TZVP basis set[62-63] for all atoms, the D3(BJ) empirical dispersion correction, and a chloroform solvent field correction. Frequency calculations were then performed on the resulting geometries to determine if they were stationary points (no imaginary frequencies) or transition states (exactly one imaginary frequency). Geometries of interest were then re-optimized with the def2-TZVPP basis set on all atoms.

Acknowledgments

G.S.G. thanks the National Science Foundation under grant CHE 19-54745 for support of this research, and the School of Chemical Sciences of the University of Illinois for computational resources. We thank Dr. Danielle Gray and Dr. Toby Woods for collecting the X-ray diffraction data, and we thank Prof. Kostas Vogiatzis and Dr. Lingyang Zhu for helpful discussions.

ASSOCIATED CONTENT

Supporting Information Available

Crystallographic studies and IR, ^{1}H, $^{13}C\{^{1}H\}$ and ^{195}Pt NMR spectra of **1**-**3**, DFT calculations of **3**, kinetic analysis of solution phase behavior of **2** and **3**, solution phase thermolysis and SCVD byproduct analysis of **3**, GI-XRD analysis of thin films grown from **3**, TGA data for **3**, and computational coordinates.

Accession Codes

CCDC 2351477, 2351482, and 2351483 contain the supplementary crystallographic data for this paper. These data can be obtained free of charge via www.ccdc.cam.ac.uk/data_request/cif, or by emailing data_request@ccdc.cam.ac.uk, or by contacting The Cambridge Crystallographic Data Centre, 12 Union Road, Cambridge CB2 1EZ, UK; fax: +44 1223 336033

AUTHOR INFORMATION

Corresponding Author

* E-mail: girolami@scs.illinois.edu (G.S.G).

Author Contributions

All authors have given approval to the final version of the manuscript.

Funding Sources

National Science Foundation under grant CHE 19-54745 (to G.S.G.).

Conflict of Interest Disclosure

The authors declare no competing financial interest.

References.

1. Pierson, H. O., Introduction and General Considerations. In *Handbook of Chemical Vapor Deposition*, Pierson, H. O., Ed. William Andrew Publishing: Oxford, 1992; pp 1-16.
2. Hampden-Smith, M. J.; Kodas, T. T., Chemical Vapor Deposition of Metals: Part 1. An Overview of CVD Processes. *Chem. Vap. Depos.* **1995,** *1*, 8-23.
3. Doppelt, P., Why is Coordination Chemistry Stretching the Limits of Micro-electronics Technology? *Coord. Chem. Rev.* **1998,** *178-180*, 1785-1809.
4. Jones, A. C.; Hitchman, M. L., Overview of Chemical Vapour Deposition. In *Chemical Vapour Deposition: Precursors, Processes and Applications*, Jones, A. C.; Hitchman, M. L., Eds. The Royal Society of Chemistry: 2008; p 0.
5. Hämäläinen, J.; Ritala, M.; Leskelä, M., Atomic Layer Deposition of Noble Metals and Their Oxides. *Chem. Mater.* **2014,** *26*, 786-801.
6. George, S. M., Atomic Layer Deposition: An Overview. *Chem. Rev.* **2010,** *110*, 111-131.
7. Bernal Ramos, K.; Saly, M. J.; Chabal, Y. J., Precursor Design and Reaction Mechanisms for the Atomic Layer Deposition of Metal Films. *Coord. Chem. Rev.* **2013,** *257*, 3271-3281.
8. Aaltonen, T.; Ritala, M.; Sajavaara, T.; Keinonen, J.; Leskelä, M., Atomic Layer Deposition of Platinum Thin Films. *Chem. Mater.* **2003,** *15*, 1924-1928.
9. Fang, Q.; Hodson, C.; Xu, C.; Gunn, R., Nucleation and Growth of Platinum Films on High-*k*/Metal Gate Materials by Remote Plasma and Thermal ALD. *Phys. Procedia* **2012,** *32*, 551-560.
10. Hiratani, M.; Nabatame, T.; Matsui, Y.; Imagawa, K.; Kimura, S., Platinum Film Growth by Chemical Vapor Deposition Based on Autocatalytic Oxidative Decomposition. *J. Electrochem. Soc.* **2001,** *148*, C524.
11. Baum, T. H.; Comita, P. B., Laser-induced Chemical Vapor Deposition of Metals for Microelectronics Technology. *Thin Solid Films* **1992,** *218*, 80-94.
12. Suga, Y. M.; Hiratani, M.; Miki, H.; Fujisaki, Y., Oxygen Diffusion in Pt Bottom Electrodes of Ferroelectric Capacitors. *Jpn. J. Appl. Phys.* **1997,** *36*, L1239.
13. Nayak, M.; Ezhilvalavan, S.; Tseng, T. Y., Chapter 2 - High-Permittivity (Ba, Sr)TiO_3 Thin Films. In *Handbook of Thin Films*, Singh Nalwa, H., Ed. Academic Press: Burlington, 2002; pp 99-167.
14. Ryan, M., PGM Highlights: Platinum in Next-Generation Materials for Data Storage. *Platinum Metals Rev.* **2010,** *54*, 244-249.
15. Hierso, J.-C.; Serp, P.; Feurer, R.; Kalck, P., MOCVD of Rhodium, Palladium and Platinum Complexes on Fluidized Divided Substrates: Novel Process for One-step Preparation of Noble-metal Catalysts. *Appl. Organomet. Chem.* **1998,** *12*, 161-172.
16. Serp, P.; Kalck, P.; Feurer, R., Chemical Vapor Deposition Methods for the Controlled Preparation of Supported Catalytic Materials. *Chem. Rev.* **2002,** *102*, 3085-3128.
17. Choi, D. S.; Robertson, A. W.; Warner, J. H.; Kim, S. O.; Kim, H., Low-Temperature Chemical Vapor Deposition Synthesis of Pt–Co Alloyed Nanoparticles with Enhanced Oxygen Reduction Reaction Catalysis. *Adv. Mater.* **2016,** *28*, 7115-7122.
18. Hsieh, C.-T.; Chen, W.-Y.; Tzou, D.-Y.; Roy, A. K.; Hsiao, H.-T., Atomic Layer Deposition of Pt Nanocatalysts on Graphene Oxide Nanosheets for Electro-oxidation of Formic Acid. *Int. J. Hydrog. Energy* **2012,** *37*, 17837-17843.

19. Liu, C.; Wang, C.-C.; Kei, C.-C.; Hsueh, Y.-C.; Perng, T.-P., Atomic Layer Deposition of Platinum Nanoparticles on Carbon Nanotubes for Application in Proton-Exchange Membrane Fuel Cells. *Small* **2009,** *5*, 1535-1538.
20. Dorovskikh, S. I.; Zharkova, G. I.; Turgambaeva, A. E.; Krisyuk, V. V.; Morozova, N. B., Chemical Vapour Deposition of Platinum Films on Electrodes for Pacemakers: Novel Precursors and their Thermal Properties. *Appl. Organomet. Chem.* **2017,** *31*, e3654.
21. Woodward, B. K., Platinum Group Metals (PGMs) for Permanent Implantable Electronic Devices. In *Precious Metals for Biomedical Applications*, Baltzer, N.; Copponnex, T., Eds. Woodhead Publishing: 2014; pp 130-147.
22. Morcos, B. M.; O'Callaghan, J. M.; Amira, M. F.; Van Hoof, C.; Op de Beeck, M., Electrodeposition of Platinum Thin Films as Interconnects Material for Implantable Medical Applications. *J. Electrochem. Soc.* **2013,** *160*, D300.
23. Liu, S.; Zhang, Z.; Abelson, J. R.; Girolami, G. S., Platinum ω-Alkenyl Compounds as Chemical Vapor Deposition Precursors. Mechanistic Studies of the Thermolysis of $Pt[CH_2CMe_2CH_2CH{=}CH_2]_2$ in Solution and the Origin of Rapid Nucleation. *Organometallics* **2020,** *39*, 3817-3829.
24. Liu, S.; Zhang, Z.; Gray, D.; Zhu, L.; Abelson, J. R.; Girolami, G. S., Platinum ω-Alkenyl Compounds as Chemical Vapor Deposition Precursors: Synthesis and Characterization of $Pt[CH_2CMe_2CH_2CH{=}CH_2]_2$ and the Impact of Ligand Design on the Deposition Process. *Chem. Mater.* **2020,** *32*, 9316-9334.
25. Lee, W.-J.; Wan, Z.; Kim, C.-M.; Oh, I.-K.; Harada, R.; Suzuki, K.; Choi, E.-A.; Kwon, S.-H., Atomic Layer Deposition of Pt Thin Films Using Dimethyl (*N*,*N*-Dimethyl-3-Butene-1-Amine-*N*) Platinum and O_2 Reactant. *Chem. Mater.* **2019,** *31*, 5056-5064.
26. Tagge, C. D.; Simpson, R. D.; Bergman, R. G.; Hostetler, M. J.; Girolami, G. S.; Nuzzo, R. G., Synthesis of a Novel Volatile Platinum Complex for Use in CVD and a Study of the Mechanism of Its Thermal Decomposition in Solution. *J. Am. Chem. Soc.* **1996,** *118*, 2634-2643.
27. Mackus, A. J. M.; Leick, N.; Baker, L.; Kessels, W. M. M., Catalytic Combustion and Dehydrogenation Reactions during Atomic Layer Deposition of Platinum. *Chem. Mater.* **2012,** *24*, 1752-1761.
28. Xue, Z.; Strouse, M. J.; Shuh, D. K.; Knobler, C. B.; Kaesz, H. D.; Hicks, R. F.; Williams, R. S., Characterization of (Methylcyclopentadienyl)trimethylplatinum and Low-temperature Organometallic Chemical Vapor Deposition of Platinum Metal. *J. Am. Chem. Soc.* **1989,** *111*, 8779-8784.
29. Xue, Z.; Thridandam, H.; Kaesz, H. D.; Hicks, R. F., Organometallic Chemical Vapor Deposition of Platinum. Reaction Kinetics and Vapor Pressures of Precursors. *Chem. Mater.* **1992,** *4*, 162-166.
30. Knoops, H. C. M.; Mackus, A. J. M.; Donders, M. E.; van de Sanden, M. C. M.; Notten, P. H. L.; Kessels, W. M. M., Remote Plasma ALD of Platinum and Platinum Oxide Films. *Electrochem. Solid-State Lett.* **2009,** *12*, G34.
31. Dendooven, J.; Ramachandran, R. K.; Devloo-Casier, K.; Rampelberg, G.; Filez, M.; Poelman, H.; Marin, G. B.; Fonda, E.; Detavernier, C., Low-Temperature Atomic Layer Deposition of Platinum Using (Methylcyclopentadienyl)trimethylplatinum and Ozone. *J. Phys. Chem. C* **2013,** *117*, 20557-20561.
32. Herbrich, T.; Thiele, K.-H.; Thewalt, U., Synthese und Molekülstruktur von $Li[(Me_2NCH_2CH_2CH_2)_4Yb]$. *Z. Anorg. Allg. Chem.* **1996,** *622*, 1609-1611.

33. Langguth, E.; Van Thu, N.; Shakoor, A.; Jacob, K.; Thiele, K.-H., Beiträge zur Chemie der Alkylverbindungen von Übergangsmetallen. XXXVI. Zur Existenz von 3(*N*,*N*-Dimethylamino)propyl-Verbindungen der 3d-Elemente und des Zirconiums. *Z. Anorg. Allg. Chem.* **1983,** *505*, 127-133.
34. Shakoor, A.; Jacob, K.; Thiele, K.-H., Beiträge zur Chemie der Alkylverbindungen von Übergangsmetallen. XXXIX. Über 3(*N*,*N*-Dimethylamino)propyllanthanoid-Verbindungen. *Z. Anorg. Allg. Chem.* **1985,** *521*, 57-60.
35. Latten, J. L.; Dickson, R. S.; Deacon, G. B.; West, B. O.; Tiekink, E. R. T., The Synthesis of Alkylmanganese(III) Complexes. Crystal structure of $MnMe(2\text{-}Me_2NCH_2C_6H_4)_2$. *J. Organomet. Chem.* **1992,** *435*, 101-108.
36. Thiele, K.-H.; Herbrich, T., Darstellung und Eigenschaften von 3-(*N*,*N*-Dimethylamino)propyl-Verbindungen des Thalliums. *Z. Anorg. Allg. Chem.* **1995,** *621*, 2025-2028.
37. Shakoor, A.; Jacob, K.; Thiele, K.-H., Beiträge zur Chemie der Alkylverbindungen von Übergangsmetallen. XXXIV. Darstellung und Eigenschaften von 3-(*N*,*N*-Dialkylamino)-propylmangan-Verbindungen. *Z. Anorg. Allg. Chem.* **1983,** *498*, 115-120.
38. Mai, L.; Mitschker, F.; Bock, C.; Niesen, A.; Ciftyurek, E.; Rogalla, D.; Mickler, J.; Erig, M.; Li, Z.; Awakowicz, P.; Schierbaum, K.; Devi, A., From Precursor Chemistry to Gas Sensors: Plasma-Enhanced Atomic Layer Deposition Process Engineering for Zinc Oxide Layers from a Nonpyrophoric Zinc Precursor for Gas Barrier and Sensor Applications. *Small* **2020,** *16*, 1907506.
39. Mai, L.; Zanders, D.; Subaşı, E.; Ciftyurek, E.; Hoppe, C.; Rogalla, D.; Gilbert, W.; Arcos, T. d. l.; Schierbaum, K.; Grundmeier, G.; Bock, C.; Devi, A., Low-Temperature Plasma-Enhanced Atomic Layer Deposition of Tin(IV) Oxide from a Functionalized Alkyl Precursor: Fabrication and Evaluation of SnO_2-Based Thin-Film Transistor Devices. *ACS Appl. Mater. Interfaces* **2019,** *11*, 3169-3180.
40. Zickgraf, A.; Beuter, M.; Kolb, U.; Dräger, M.; Tozer, R.; Dakternieks, D.; Jurkschat, K., Nucleophilic Attack within Ge, Sn and Pb Complexes Containing $Me_2N(CH_2)_3$—as a Potential Intramolecular Donor Ligand. *Inorg. Chim. Acta* **1998,** *275-276*, 203-214.
41. Deis, T.; Maury, J.; Medici, F.; Jean, M.; Forte, J.; Vanthuyne, N.; Fensterbank, L.; Lemière, G., Synthesis and Optical Resolution of Configurationally Stable Zwitterionic Pentacoordinate Silicon Derivatives. *Angew. Chem. Int. Ed.* **2022,** *61*, e202113836.
42. Göttker-Schnetmann, I.; Mecking, S., A Practical Synthesis of $[(tmeda)Ni(CH_3)_2]$, Isotopically Labeled $[(tmeda)Ni(^{13}CH_3)_2]$, and Neutral Chelated-Nickel Methyl Complexes. *Organometallics* **2020,** *39*, 3433-3440.
43. De Graaf, W.; Boersma, J.; Smeets, W. J. J.; Spek, A. L.; Van Koten, G., Dimethyl(*N*,*N*,*N*',*N*'-tetramethylethanediamine)palladium(II) and Dimethyl[1,2-bis(dimethylphosphino)ethane]palladium(II): Syntheses, X-ray Crystal Structures, and Thermolysis, Oxidative-addition and Ligand-exchange Reactions. *Organometallics* **1989,** *8*, 2907-2917.
44. Lastowski, R. J.; Girolami, G. S., Dimethyl(*N*,*N*,*N*',*N*'-tetramethylethylenediamine)platinum(II). *IUCrData* **2024,** *In press*.
45. Reich, H. J., WinDNMR: Dynamic NMR Spectra for Windows. *J. Chem. Educ.* **1995,** *72*, 1086.
46. Whitesides, G. M.; Hackett, M.; Brainard, R. L.; Lavalleye, J. P. P. M.; Sowinski, A. F.; Izumi, A. N.; Moore, S. S.; Brown, D. W.; Staudt, E. M., Suppression of Unwanted Heterogeneous Platinum(0)-catalyzed Reactions by Poisoning with Mercury(0) in Systems Involving Competing

Homogeneous Reactions of Soluble Organoplatinum Compounds: Thermal Decomposition of Bis(triethylphosphine)-3,3,4,4-tetramethylplatinacyclopentane. *Organometallics* **1985,** *4*, 1819-1830.
47. Jeffries, P. M.; Dubois, L. H.; Girolami, G. S., Metal-organic Chemical Vapor Deposition of Copper and Copper(I) Oxide from Copper(I)*tert*-butoxide. *Chem. Mater.* **1992,** *4*, 1169-1175.
48. Girolami, G. S., Quantitative analysis of the initial protons remaining in the CVD products of **3** was not performed due to incomplete volatilization of the initial sample of **3**.
49. Alexanian, E. J.; Hartwig, J. F., Mechanistic Study of β-Hydrogen Elimination from Organoplatinum(II) Enolate Complexes. *J. Am. Chem. Soc.* **2008,** *130*, 15627-15635.
50. Romeo, R.; Alibrandi, G.; Scolaro, L. M., Kinetic Study of β-Hydride Elimination from Monoalkyl Solvento Complexes of Platinum(II). *Inorg. Chem.* **1993,** *32*, 4688-4694.
51. Ng, S. M.; Zhao, C.; Lin, Z., Theoretical Studies on the β-Hydrogen Elimination Reactions of Palladium and Platinum Alkoxide Complexes Containing Bidentate Ligands. *J. Organomet. Chem.* **2002,** *662*, 120-129.
52. Garcia, J. R. V.; Goto, T., Chemical Vapor Deposition of Iridium, Platinum, Rhodium and Palladium. *Mater. Trans.* **2003,** *44*, 1717-1728.
53. Gibbs, C. F.; Littmann, E. R.; Marvel, C. S., Quaternary Ammonium Salts from Halogenated Alkyl Dimethylamines. II. The Polymerization of Gamma-Halogenopropyldimethylamines. *J. Am. Chem. Soc.* **1933,** *55*, 753-757.
54. Davis, L. M. Syntheses, Properties, and Reactions of Transition Metal Complexes of Di(*tert*-butyl)amide and 2,2,6,6-Tetramethylpiperidide. University of Illinois at Urbana-Champaign, 2014.
55. Berton, G.; Lorenzetto, T.; Borsato, G.; Sgarbossa, P.; Santo, C.; Visentin, F.; Fabris, F.; Scarso, A., Triphenylene Based Metal-Pyridine Cages. *Tetrahedron Lett.* **2019,** *60*, 151202.
56. McDermott, J. X.; White, J. F.; Whitesides, G. M., Thermal Decomposition of Bis(phosphine)platinum(II) Metallocycles. *J. Am. Chem. Soc.* **1976,** *98*, 6521-6528.
57. Siegel, J. S.; Anet, F. A. L., Dichlorofluoromethane-d: A Versatile Solvent for VT-NMR Experiments. *J. Org. Chem.* **1988,** *53*, 2629-2630.
58. Morse, P. M.; Spencer, M. D.; Wilson, S. R.; Girolami, G. S., A Static Agostic α-CH···M Interaction Observable by NMR Spectroscopy: Synthesis of the Chromium(II) Alkyl $[Cr_2(CH_2SiMe_3)_6]^{2-}$ and Its Conversion to the Unusual "Windowpane" Bis(metallacycle) Complex $[Cr(\kappa^2\text{-}C,C'\text{-}CH_2SiMe_2CH_2)_2]_2$. *Organometallics* **1994,** *13*, 1646-1655.
59. Frisch, M. J.; Trucks, G. W.; Schlegel, H. B.; Scuseria, G. E.; Robb, M. A.; Cheeseman, J. R.; Scalmani, G.; Barone, V.; Petersson, G. A.; Nakatsuji, H.; Li, X.; Caricato, M.; Marenich, A. V.; Bloino, J.; Janesko, B. G.; Gomperts, R.; Mennucci, B.; Hratchian, H. P.; Ortiz, J. V.; Izmaylov, A. F.; Sonnenberg, J. L.; Williams; Ding, F.; Lipparini, F.; Egidi, F.; Goings, J.; Peng, B.; Petrone, A.; Henderson, T.; Ranasinghe, D.; Zakrzewski, V. G.; Gao, J.; Rega, N.; Zheng, G.; Liang, W.; Hada, M.; Ehara, M.; Toyota, K.; Fukuda, R.; Hasegawa, J.; Ishida, M.; Nakajima, T.; Honda, Y.; Kitao, O.; Nakai, H.; Vreven, T.; Throssell, K.; Montgomery Jr., J. A.; Peralta, J. E.; Ogliaro, F.; Bearpark, M. J.; Heyd, J. J.; Brothers, E. N.; Kudin, K. N.; Staroverov, V. N.; Keith, T. A.; Kobayashi, R.; Normand, J.; Raghavachari, K.; Rendell, A. P.; Burant, J. C.; Iyengar, S. S.; Tomasi, J.; Cossi, M.; Millam, J. M.; Klene, M.; Adamo, C.; Cammi, R.; Ochterski, J. W.; Martin, R. L.; Morokuma, K.; Farkas, O.; Foresman, J. B.; Fox, D. J. *Gaussian 16 Rev. C.01*, Wallingford, CT, 2016.
60. Becke, A. D., Density-Functional Thermochemistry. III. The Role of Exact Exchange. *J. Chem. Phys.* **1993,** *98*, 5648-5652.

61. Lee, C.; Yang, W.; Parr, R. G., Development of the Colle-Salvetti Correlation-energy Formula into a Functional of the Electron Density. *Phys. Rev. B* **1988,** *37*, 785-789.
62. Weigend, F.; Ahlrichs, R., Balanced Basis Sets of Split Valence, Triple Zeta Valence and Quadruple Zeta Valence Quality for H to Rn: Design and Assessment of Accuracy. *Phys. Chem. Chem. Phys.* **2005,** *7*, 3297-3305.
63. Andrae, D.; Häußermann, U.; Dolg, M.; Stoll, H.; Preuß, H., Energy-adjusted ab initio Pseudopotentials for the Second and Third Row Transition Elements. *Theor. Chim. Acta* **1990,** *77*, 123-141.
64. Grimme, S., Semiempirical Hybrid Density Functional with Perturbative Second-order Correlation. *J. Chem. Phys.* **2006,** *124*.
65. Johnson, E. R.; Becke, A. D., A Post-Hartree-Fock Model of Intermolecular Interactions: Inclusion of Higher-order Corrections. *J. Chem. Phys.* **2006,** *124*.
66. Barone, V.; Cossi, M., Quantum Calculation of Molecular Energies and Energy Gradients in Solution by a Conductor Solvent Model. *J. Phys. Chem. A* **1998,** *102*, 1995-2001.